Measurement Science and Technology

Best Paper Award 2003

IS PRESENTED TO:

Richard Hafer and Arno Laesecke
Atmel Corp, Colorado, USA; National Institute of Standards and Technology, Boulder, USA

FOR THE ARTICLE:

Extension of the torsional crystal viscometer to measurements in the time domain

Measurement Science and Technology
Volume 14 663-673 (2003)

Professor Peter Hauptmann
Editor-in-Chief
Measurement Science and Technology

Institute *of* **Physics** PUBLISHING

INSTITUTE OF PHYSICS PUBLISHING MEASUREMENT SCIENCE AND TECHNOLOGY

Meas. Sci. Technol. **14** (2003) 663–673 PII: S0957-0233(03)39287-2

Extension of the torsional crystal viscometer to measurements in the time domain

Richard F Hafer[1] **and Arno Laesecke**[2]

National Institute of Standards and Technology, Chemical Science and Technology Laboratory,
Physical and Chemical Properties Division, Experimental Properties of Fluids Group,
325 Broadway, Boulder, CO 80305-3328, USA

E-mail: Arno.Laesecke@Boulder.NIST.Gov

Received 9 July 2002, in final form 20 February 2003,
accepted for publication 12 March 2003
Published 15 April 2003
Online at stacks.iop.org/MST/14/663

Abstract
This paper reports the first wide-ranging application of the free-mode measurement technique to a torsional crystal viscometer. The viscous damping of the fluid on the surface of the crystal is detected in the time domain by observing the freely decaying torsional oscillation of the crystal. Previously, the torsional crystal viscometer was used exclusively in a forced mode of measurement, where the response of the crystal is determined in the frequency domain by scanning through the resonance.

The free-decay measurement mode has many advantages over the previous technique. It enables a better characterization of the sensor because the torsional displacement of the crystal can be observed directly. Measurements can be carried out at smaller displacements as well as at constant amplitude in fluid and *in vacuo*. Direct control over the crystal displacement is an important extension (especially at low external damping of the crystal as in gases or *in vacuo*), because the measurements can be limited to the linear regime of the crystal vibration and the nonlinear regime can be avoided. In addition, this extension allows for a more complete characterization of the transducer by validating the consistency of its operation in the time and frequency domains. Finally, free-decay measurements are much faster than resonance scans, thus eliminating medium and large time constant variables that can affect the measurement. With these advantages, a second metrological approach has been added to the utilization of torsional crystal viscometers.

Sulfur hexafluoride (SF_6) was used as a test fluid to compare the two measurement modes in the presence of external damping. The results of both methods are consistent up to a (viscosity $\times$ density) of 0.020 (Pa s)(kg m^{-3}). With improved signal conditioning this limit can be increased substantially.

Both measurement techniques were also compared to determine the internal damping of the crystal *in vacuo*. Nonlinear crystal oscillations were observed which can be interpreted in terms of Duffing and Van der Pol nonlinearities with displacement-dependent stiffness and damping respectively. This insight represents a substantial advance in our understanding of torsional crystal viscometers.

Keywords: torsional crystal viscometer, sulfur hexafluoride, viscosity, transient decay, free mode measurement, rapid data acquisition, nonlinear oscillations

(Some figures in this article are in colour only in the electronic version)

1. Introduction

Torsionally vibrating cylindrical piezoelectric crystal rods have been employed for shear viscosity measurements of fluids. Figure 1 illustrates schematically the oscillatory velocity field that is generated by such vibrators. The measured damping of the vibrator yields the information used to deduce the viscosity of the surrounding fluid.

Such viscometers have been used for a wide range of measurements from gas to polymer viscosities, low to high temperatures, and to high pressures. Kestin and Wakeham [1], Diller [2], and Meyer [3] reviewed many applications of the technique since its conception in 1947. Later, Gundrum [4]

[1] Present address: Atmel Corp., 1150 E. Cheyenne Mtn. Blvd., Colorado Springs, CO 80906, USA.
[2] Author to whom any correspondence should be addressed.

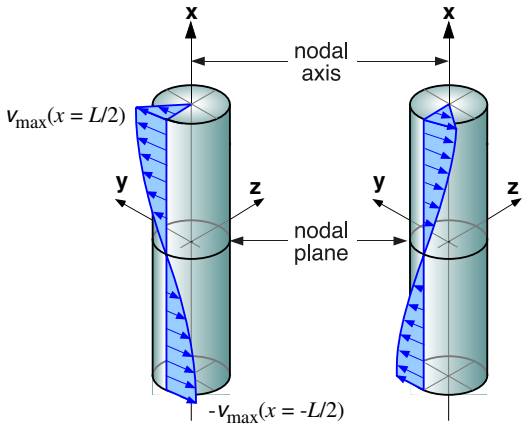

Figure 1. Velocity field generated on the surface of the quartz crystal by the torsional vibration of the cylindrical rod. The crystal is shown at zero torsional displacement when the velocity at its surface reaches a maximum. Ideally, no displacement occurs along the x-axis or in the nodal plane.

extended the upper temperature limit to 623 K by using swept quartz crystals [5] while Meier [6] analysed the torsional crystal vibration in terms of equivalent electric circuits and investigated the effect of fluid polarity on the measured response of the piezoelectric crystal.

As with every vibrating system, the damping on the torsionally vibrating crystal can be measured in two ways. The predominant measuring mode for torsional crystal viscometers has been that of mechanical spectroscopy in the frequency domain. In that mode, the damping is obtained by measuring the response of the vibrator to frequency modulations around its resonance (forced mode). Ideally, the same damping should be obtained by directly monitoring the decaying amplitude of the vibration in the absence of a driving force (free mode). This approach was attempted with torsional crystal viscometers as early as 1958 [7], and was continued in the following decade by Betts and co-workers [8–11]. These early investigations suffered primarily from slow data acquisition capabilities. In these works, as in unpublished attempts during helium measurements in this laboratory [12], the decaying crystal vibration was photographed from an oscilloscope screen for quantitative evaluation of the damping constant. The limitations of this data acquisition method are obvious considering the high resonant frequencies of torsionally vibrating crystals of typically 40 kHz and the rapid decay of their oscillations in the presence of liquids. No other attempts to deduce viscosities from free decay measurements have been reported since 1972.

Here, we present the quantitative implementation of the measurement mode where the decay of the crystal vibration is monitored in the time domain. Throughout this paper, the terms 'free mode' and 'free decay' refer to the time-domain measurements, and the terms 'forced mode' and 'resonance scan' are synonymous for frequency-domain measurements. Following introductory theoretical considerations about the equivalence of the two measurement modes, the main features of the employed viscometer and the hardware implementation for the free-mode measurement are described. The data analysis of free-decay measurements will be discussed and sample results *in vacuo* and in sulfur hexafluoride will be presented. The new measurement method revealed nonlinear vibrational behaviour of the quartz crystal, which is interpreted in the final part of this paper.

2. Working theory for both measurement modes

The forced-mode and the free-mode technique both attempt to measure the viscous damping of a fluid on the crystal surface by determining the logarithmic decrement of the crystal vibration. In resonance-scan measurements, it is obtained by measuring the response of the vibrating crystal to variations of the drive frequency near its resonance and determining from that the resonant frequency (f^*) and half-power bandwidth (Δf) of the resonance curve. For such systems, 'resonance' is defined by the physical properties of the system (mass and elasticity); and for real systems (which always include damping) this corresponds to the frequency of maximum power dissipation. The half-power points are the two frequencies where the dissipated power is half that of the maximum. In the time domain (free-mode measurement), the damping is determined by direct observation of the decaying amplitude of the crystal oscillation.

The working equation for absolute viscosity measurements in the forced mode was derived in detail by Webeler [13] and Meier [6]:

$$\eta \times \rho = \left(\frac{m}{S}\right)^2 (\pi f^*)\left(\frac{\Delta f}{f^*} - \frac{\Delta f_0}{f_0^*}\right)^2. \qquad (1)$$

Here, η represents the viscosity of the fluid, ρ its density, m the mass, S the surface area of the crystal, f^* the resonant frequency and Δf the bandwidth. The subscript 0 indicates vacuum conditions. Other working equations have been proposed, where the viscosity of the fluid is deduced only from the resonant frequency shift between vacuum and fluid [14–16]. It was found that these working equations are not suitable for absolute viscosity measurements.

The working equation to obtain the product (viscosity × density) from the free decay of the crystal vibration is [11]

$$\eta \times \rho = \left(\frac{m}{S}\right)^2 \left(\frac{f^*}{\pi}\right)(\chi - \chi_0)^2, \qquad (2)$$

where χ is the logarithmic decrement of the free decay. This equation is equivalent to equation (1) with the substitution

$$\chi = \pi \frac{\Delta f}{f^*}. \qquad (3)$$

Equation (2) was adopted as the working equation for the free-decay viscosity measurements in this work.

There are three different frequencies characterizing the frequency response of a damped system. These are (1) the 'undamped natural frequency', (2) the 'damped natural frequency' and (3) the 'frequency of maximum forced amplitude'. The derivation of these frequencies may be found in reference textbooks on acoustics or vibrations, such as those by Kinsler *et al* [17] or den Hartog [18]. The difference between the three frequencies is extremely small for piezoelectric quartz crystals even at the highest measurable

damping, where it amounts to about 100 mHz at an operating frequency of approximately 40 kHz. Thus, the frequency difference is negligible in the calculation of the viscosity according to equation (1) or (2), and throughout this paper no distinction between the damped and the undamped natural frequencies will be made. The term 'resonant frequency' will be used throughout.

Since this technique measures the product ($\eta \times \rho$), the density of the fluid must be known in order to extract its viscosity. Densities are obtained either from an equation of state or from experimental data. The uncertainty in the density thus affects the uncertainty of the reported viscosity.

3. Experimental details

3.1. Apparatus and implementation

The free-decay measurement technique was implemented in the low-temperature viscometer as shown schematically in figure 2. The instrument can be operated in a temperature range from 60 to 330 K at pressures from vacuum to 35 MPa. In the present work, experiments *in vacuo* and with helium were carried out from 78 to 330 K. The bulk of the measurements were carried out on sulfur hexafluoride (SF_6) from 225.18 K near its triple point to 325.60 K slightly above the critical point, and at pressures from 0.0923 to 34.47 MPa. The transducer with the quartz crystal is enclosed in a beryllium + copper pressure vessel. The cylindrical quartz crystal (designated WMH1) has a mass of 2.5121 ± 0.0002 g, a length of 49.9008 ± 0.006 mm, and a diameter of 4.920 ± 0.006 mm. The surface area is thus 8.093 ± 0.011 cm^2. The mass has been measured to 0.01% and the surface area to 0.1%. The surface area is further corrected for thermal expansion and pressure effects at the experimental conditions. The resonant frequency of the crystal is 39.461 06 kHz *in vacuo* at 298.15 K. It depends inversely on the length of the crystal. Knowledge of its variation with temperature is a necessary prerequisite for absolute viscosity measurements with this instrument.

The implementation of the free-mode technique required no modification of the transducer itself, but only additions to the data acquisition instrumentation outside the cryostat. While the crystal is forced to vibrate torsionally when an ac voltage is applied to its surrounding electrodes (converse piezoelectric effect), the free decay of the crystal vibration can be measured by recording the voltage that is induced in the electrodes proportional to the crystal deformation (piezoelectric effect). Therefore, the additional hardware components include a triggered relay, a fast analogue-to-digital (A/D) data acquisition board, and an intermediate amplifier. The triggered relay serves the purpose of switching the electrodes of the transducer from the driving impedance analyser to the A/D board, and the amplifier increases the signal strength during measurements in compressed fluids and liquids. These modifications are indicated in figure 2.

An alternative way of measuring the free decay of the crystal vibration is by using a lock-in amplifier. In this bead frequency technique, the measured signal is superimposed to a reference signal in what could be considered as analogue preprocessing to reduce the amount of digital data. The objective of this work was to explore a fully digital technique because it was anticipated that the limits of data acquisition and processing speed, memory demand and storage capacity would relax soon. The fully digital technique can be realized with very compact data acquisition that offers the possibility of developing this viscometer into a portable instrument for field use, such as down-hole measurements in oil reservoirs.

3.2. Prerequisites for free-decay measurements

The forced-mode technique has been the primary method of determining the fluid damping on the crystal surface in the torsional crystal viscometer since 1947. Initially, such measurements were carried out with radio bridges by manually determining the resonance frequency and the half-power point frequencies. The shape of the resonance was not fully resolved and nonlinearities remained undetected. When impedance analysers became available, it was possible to measure a resonance curve completely instead of only three points of interest. This work represents the first quantitative implementation of the free-mode method in the torsional crystal viscometer. Free-decay measurements require different resources for accurate data acquisition and analysis than resonance scans. Due to the resonant frequency of the crystal at approximately 40 kHz, the decay of the crystal vibration has to be recorded with a data acquisition sampling rate of at least 2 million voltage samples per second (MS s^{-1}), so that each cycle is resolved with 50 data samples. The induced voltage is the measured quantity. *In vacuo*, measurement durations of 50 s or more are needed to observe the decay to approximately 95% of the maximum amplitude. Such a measurement at a sampling rate of 2 MS s^{-1} and a resolution of 12 bits/sample, generates a data volume of approximately 147 Mb, which has to be analysed to obtain the damping constant of the decay.

Hardware with such data recording and processing capabilities became available in the mid-1990s at an acceptable cost. A 1012 PCI data acquisition board by GaGe Applied Sciences Inc. was used to record the induced voltages[3]. Although the board is capable of rapid data acquisition, its implementation into the data acquisition system was involved. The transfer of the recorded data from the add-on board to the computer during a measurement requires an interface with a sufficiently high peripheral data-transfer rate such as the PCI bus. Finally, the data storage and analysis requires a processor with significant computational speed. Computer memory (RAM), disk space, and processor speed are critical in recording and storing several megabytes of decay data, and in their analysis to determine the damping constant.

A Pentium II processor with a clock speed of 200 MHz and 128 Mb of RAM was used as the data acquisition computer. Software limitations reduced the practical amount of data which could be recorded in a single experiment to a measurement duration of 7.5 s. While this duration was sufficient to record decays in liquids and even dilute gases, complete decays *in vacuo* could not be captured at once. Instead, multiple experiments with different initial drive

[3] In order to describe materials and experimental procedures adequately, it is occasionally necessary to identify commercial products by manufacturers' names or labels. In no instance does such identification imply endorsement by the National Institute of Standards and Technology, nor does it imply that the particular product or equipment is necessarily the best available for the purpose.

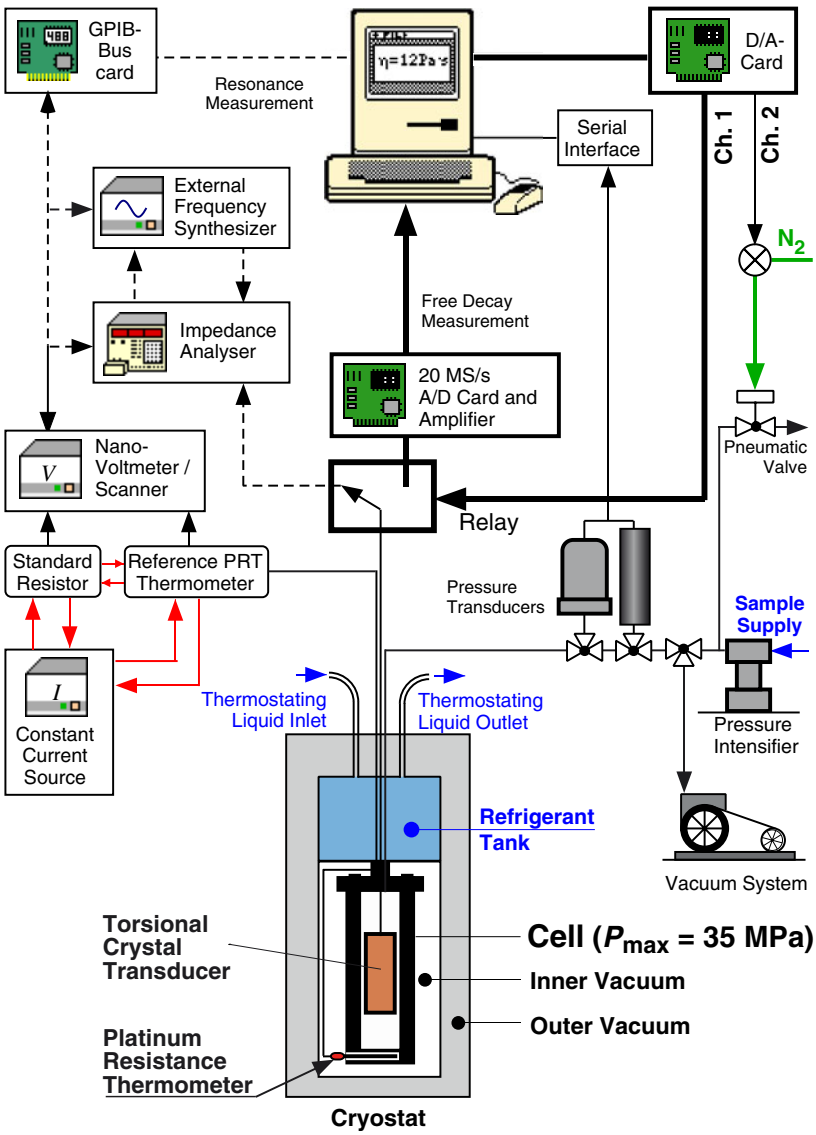

Figure 2. Schematic diagram of low-temperature viscometer for temperatures from 60 to 330 K and maximum pressures of 35 MPa. Equipment in the bold lined circuit was added for the free-decay measurement. Resonance measurements are carried out with the equipment in the dashed circuit.

voltages (amplitudes) were carried out to infer the behaviour of the vibrating crystal over the entire decay.

3.3. Data analysis

The data analysis for either measurement with the torsional crystal viscometer extracts the resonant frequency and the system damping (either in terms of bandwidth Δf or logarithmic decrement χ) from the experimental data. These values are then used in the calculation of the product $(\eta \times \rho)$ according to equations (1) and (2).

A sample resonance scan is presented in figure 3 where the dissipated power of the oscillator was measured as a function of frequency. With our instrumentation, the complex admittance Y of the crystal is measured as a function of frequency, with conductance G being the real part and susceptance B being the imaginary part, $Y = G + \mathrm{j}B$. The resonant frequency f^* is the frequency where G has a maximum ($G_{\max}$). The bandwidth Δf is determined by linear interpolation between data points around $G_{1/2}$ (the value of G that is one half of $G_{\max}$). Equation (1) is then used to determine the product $(\eta \times \rho)$.

As mentioned in section 3.2, the analysis of the data from a free-decay measurement was computationally demanding at the time when this work was carried out. Sample recordings of decays in SF_6 and *in vacuo* are shown in figures 4 and 5. The measured quantity is the piezoelectrically induced voltage in the transducer electrodes as a function of time. This signal is proportional to the torsional displacement of the crystal. Figure 4 shows the response of the transducer in supercritical SF_6 at approximately 325 K, while figure 5 shows a decay *in vacuo* without external damping at the same temperature.

For the purpose of this initial investigation, a two-step data-analysis procedure was chosen. First, the decay data were analysed with a peak-detection algorithm to determine the maxima and minima of the induced voltage. This is illustrated in figure 6 for a magnified portion of the SF_6 decay shown in

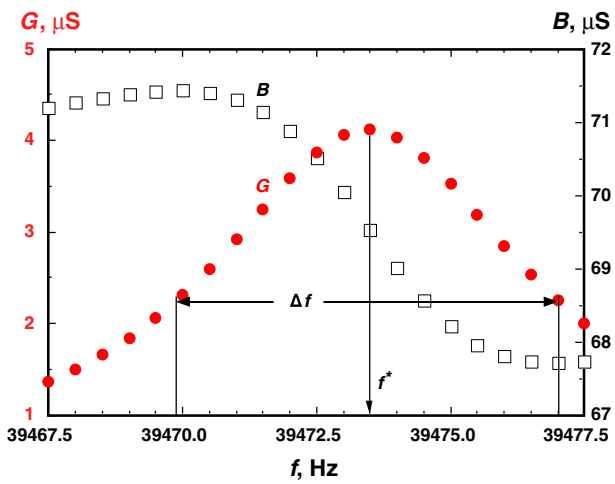

Figure 3. Crystal resonance recorded in supercritical sulfur hexafluoride (SF_6) at 325 K and 4.3 MPa. Shown are the the conductance G and the susceptance B with the resonant frequency f^* and the bandwidth Δf.

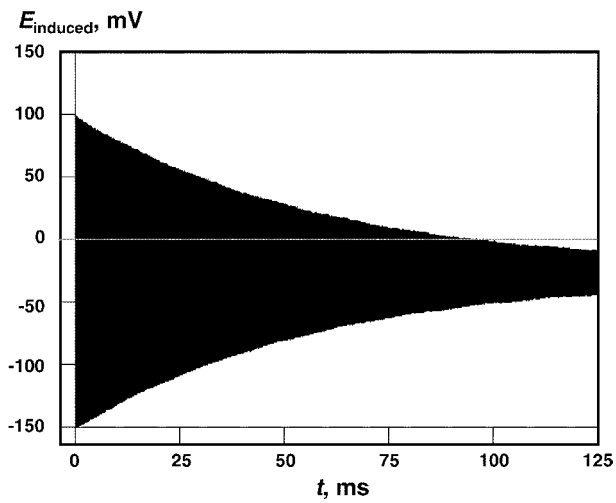

Figure 4. Free decay of the torsional crystal vibration recorded in supercritical SF_6 at 325 K and 4.3 MPa. Shown are 250 000 data points which are not discernible individually. The drive voltage was 150 mV before the decay was triggered and the induced voltages were amplified by a factor of 5.52.

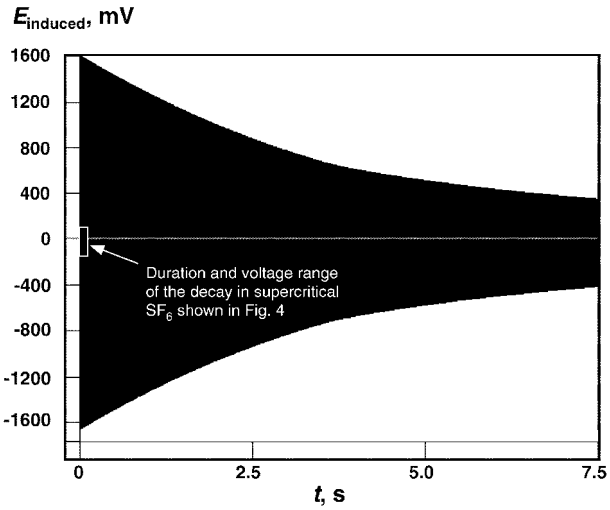

Figure 5. Free decay of the torsional crystal vibration *in vacuo* at 325 K. Shown are 15 million data points which are not discernible individually. The drive voltage was 1.1 V before the decay was triggered. The induced voltages were not amplified. Nonlinear effects are apparent in the first 4 s of the decay.

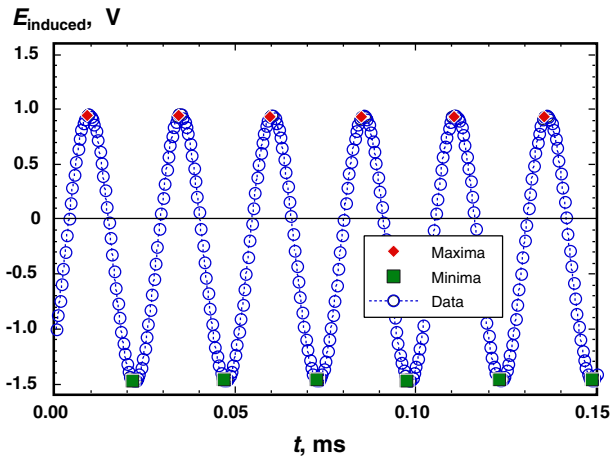

Figure 6. Analysis of free-decay data for a measurement in SF_6 at 325 K and 4.3 MPa as shown in figure 4. The data are analysed in a first step by detecting the maxima and minima of the induced voltages. The drive voltage was 1.1 V before the decay was triggered, and the induced voltages were amplified by a factor of 5.52.

figure 4. The maxima and minima of the induced voltage were averaged per cycle to find the set of cyclic amplitudes, which were in turn fitted to an exponential decay function to determine the damping coefficient β. An example of the agreement between experimental data and correlation is shown in figure 7. Each measurement was analysed by sequentially taking parcels of decay data and treating them separately. This allowed the observation of the damping coefficient as a function of time. The resonant frequency and the logarithmic decrement χ were then used with equation (2) to obtain the product $(\eta \times \rho)$.

4. Results

4.1. Vacuum measurements

Absolute viscosity measurements with the torsional crystal viscometer require an accurate characterization of the internal damping of the crystal *in vacuo*, i.e. the bandwidth Δf_0 and resonant frequency f_0^* which appear in the working equations (1) and (2). In gases with a low $(\eta \times \rho)$, the contribution of the internal damping becomes appreciable relative to the external damping by the fluid and cannot be neglected, as is often done in the analysis of measurements of liquids.

Resonance scans *in vacuo* and at low external damping deal with inherent difficulties. These consist of:

(i) considerable ring-down times $\Delta t_{\Delta f}$ which have to be allowed after a frequency step before the admittance is measured and

(ii) an increased sensitivity to the drive voltage E_{osc} which should be as low as possible.

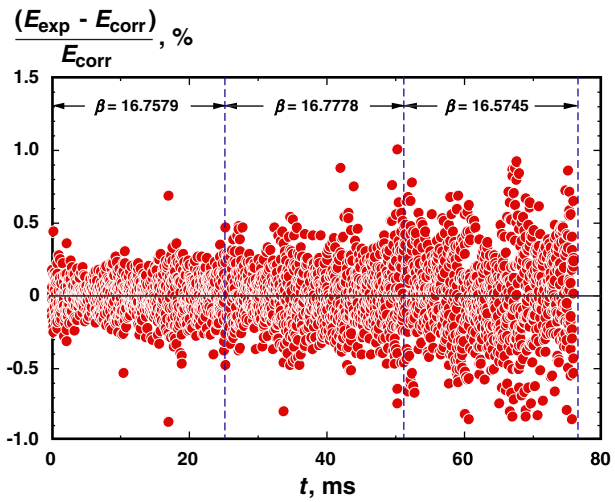

Figure 7. Deviation between exponential fit and free-decay data during 3000 cycles recorded in supercritical SF_6 at 325 K and 4.3 MPa. Other conditions as in figure 4.

These difficulties are amplified at cryogenic temperatures when the quality factor of the crystal is much higher than at ambient or higher temperatures. Figure 8 shows as an example the resonance of crystal WMH1 at 75.896 ± 0.001 K which was resolved in this work for the first time at such low temperatures. The measurement was carried out with a ring-down time of $\Delta t_{\Delta f} = 270$ s before the admittance Y was recorded after each frequency step of $\Delta f = 1$ mHz. Even if the measurement were to have been limited to the immediate frequency range around the resonance as indicated in figure 8, the execution of the scan would have lasted more than an hour. Temperature fluctuations of the thermostating system may affect such measurements so that the resonant frequency shifts with time. Such a shift can also result from a temperature rise of the crystal due to the internal dissipation of the applied power. Consequently, forced-mode measurements can yield incorrectly shaped response curves and even multiple 'resonances'. For example, the bandwidth of the resonance in figure 8 is approximately 2 mHz. Even if the resonance frequency f_0^* shifts during a resonance scan by only 1 mHz (in this case 50% of the true bandwidth), the measurement of this narrow bandwidth is considerably compromised. Note that this shift in resonant frequency is not due to a different measurement technique (i.e. forced mode versus free mode, see section 2), but rather due to non-idealities in the system. This long-time shift in resonant frequency is avoided entirely by the free-decay measurement, which takes less than a minute in the case shown in figure 8.

Another limitation of resonance measurements is the identification of nonlinear vibrations of the crystal. These depend on the applied drive voltage during a scan. The present transducer exhibits nonlinear behaviour at drive voltages as low as 100 mV. To measure nonlinearities, scans with different drive voltages have to be executed. Besides being very time consuming this was not possible to the required extent with the impedance analyser that has been used for such measurements because the resolution with which the device measures conductance and susceptance is tied to the applied drive voltage. The lower the drive voltage, the lower the

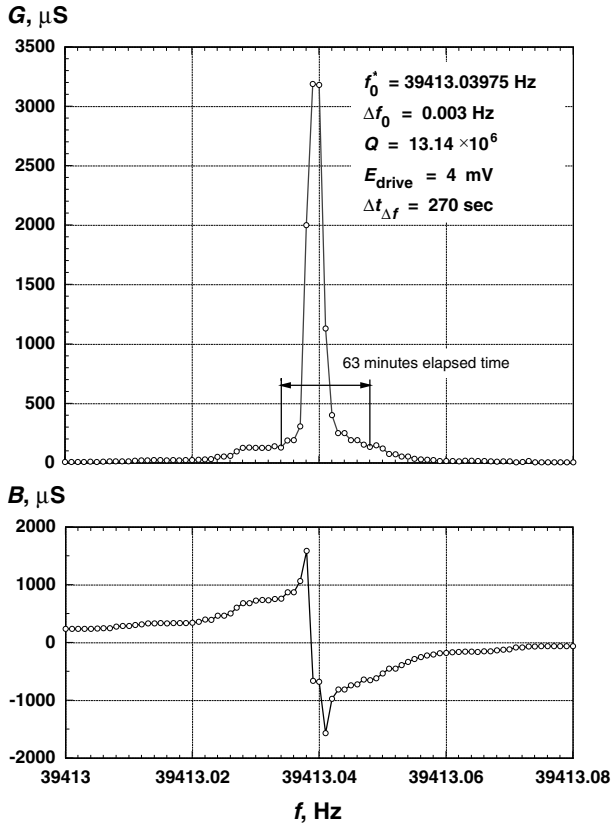

Figure 8. Resonance of crystal WMH1 *in vacuo* at 75.896 ± 0.001 K.

resolution. Due to its high quality factor, resonances of the torsionally vibrating crystal in moderately dense gases and *in vacuo* fall in a range that requires low drive voltage at sustained resolution to avoid nonlinear contributions. The free-decay measurement circumvents this limitation as it can be used in the present set-up down to 1 mV induced voltage, well within the linear regime of the operation of the instrument.

As discussed in the previous two paragraphs, forced-mode measurements at low external damping and *in vacuo* are demanding (especially at low temperatures) and an alternative measurement method is desired which avoids time- and amplitude-dependent effects. The free-decay technique overcomes both of these limitations. The example in figure 5 shows how the vacuum decay reduces the measurement time to the order of seconds.

Results of free-decay measurements *in vacuo* at 325 K are summarized in figures 9 and 10, showing the logarithmic decrement χ_0 and the resonant frequency of the free decay, f_0^*, versus the induced voltage E. Each series represents a decay measurement of 7.5 s duration with each data point based on the analysis of one half-second parcel of decay data. The decays were measured with drive voltages (initial amplitudes) between 5 mV and 1.1 V. Figure 9 shows the internal damping of the crystal as a function of induced voltage E. The damping χ_0 begins to increase strongly with the amplitude of the torsional vibration above induced voltages of 200 mV, corresponding to initial drive voltages between 30 mV and 0.1 V. This increase is indicative of nonlinear effects which are not covered by the linear theory of the instrument. A similar behaviour is observed

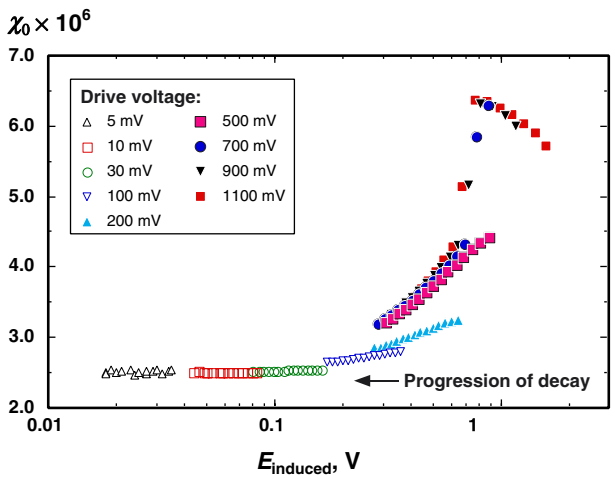

Figure 9. Internal damping of the crystal as obtained from free-decay measurements *in vacuo* at 325 K. Each data series represents one continuous measurement over 7.5 s. Each data point represents 0.5 s of a free-decay measurement. Nonlinear responses occur as the forcing of the crystal increases.

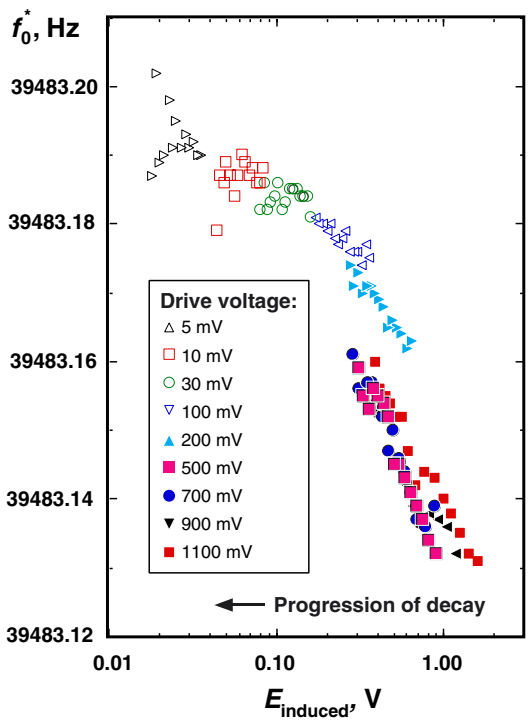

Figure 10. Free-decay resonant frequencies *in vacuo* at 325 K for the measurements shown in figure 9.

in the dependence of the resonant frequency f_0^* on the induced voltage E in figure 10. Above a certain induced voltage, the resonant frequency decreases. An explanation of the increase in damping and the change in resonant frequency in terms of nonlinear oscillators is offered in section 5. The noteworthy insight is gained with these experiments in the range of induced voltages below 0.2 V where the damping does not vary with the amplitude. Compared with forced-mode measurements, this range can be resolved by free-decay measurements with greater precision and independent of hardware constraints between drive voltage and impedance resolution limits.

4.2. Measurements in sulfur hexafluoride

Sulfur hexafluoride (SF_6) was selected as a test fluid to validate the free-decay measurement technique under external damping. Although both compounds differ in their molecular architecture, SF_6 has, like carbon dioxide, a comparably narrow vapour–liquid coexistence region between the triple and critical point ($T_t = 223.554$ K [19], $T_c = 318.729$ K [20]), so that fluid states from dilute gas to compressed liquid and supercritical fluid could be explored comprehensively in one instrument. Viscosity measurements were carried out in both modes over a temperature range from 225 to 325 K with pressures up to 35 MPa. The full set of experimental data is reported elsewhere [21].

A comparison revealed agreement within ±2% at densities above 1200 kg m^{-3} between the viscosities deduced from the resonance measurements and those literature data that were deemed most reliable. The uncertainty of the resonance-scan measurements was evaluated according to the procedure of Taylor and Kuyatt [22]. From observing the deviation of the data from the average at a state point for densities greater than 100 kg m^{-3}, a type A standard uncertainty of 1% was deduced. The type A uncertainty is associated with the precision of the instrument. 'Precision' denotes the error inherent in the instrument and measurement technique in producing repeatable results. Type B uncertainties of 0.5% for the density and 1% for systematic deviations are assumed. The type B uncertainty characterizes the accuracy of the instrument as an estimate of the error of the measured value from the true value due to systematic deviations. This evaluation gives a relative combined standard uncertainty of 1.5% for the resonance-scan SF_6 measurements in the torsional crystal viscometer. With a coverage factor of 2, the expanded relative uncertainty is ±3% for densities greater than 100 kg m^{-3}.

The free-decay measurements can be evaluated similarly. The type A uncertainty of these data is similar to that of the forced-mode data, but the free-decay data are systematically 6% lower than the corresponding resonance-scan data at an upper (viscosity × density) product $(\eta \times \rho)_{max}$ of 0.020 (Pa s) (kg m^{-3}).

A comparison between the two methods is shown in figure 11 along a supercritical isotherm at 325 K for SF_6. The results indicate that the new method is successful in determining the viscous damping on the crystal surface. The free-decay measurement data are systematically lower at higher damping due to an inability to properly quantify the damping coefficient β. The aforementioned limit of $(\eta \times \rho)_{max}$ corresponds for SF_6 to a state point of 325 K and 4.3 MPa, with a density of 767 kg m^{-3} and a viscosity of 34.7 μPa s. This is far below the present forced-mode measurement range of approximately 30 (Pa s) (kg m^{-3}). It is believed that the deteriorating performance of the free-decay measurement technique under increased external damping is mainly due to a decreasing signal to noise ratio with the present data acquisition system. The recording of the induced voltages can be improved with a low-noise switching mechanism, an improved amplifier, and better signal transmission from the transducer in the pressure vessel to the data acquisition board in the computer. Further noise reduction is possible by

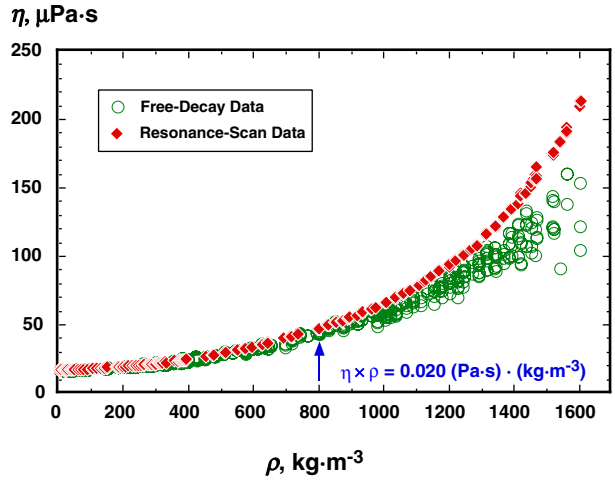

Figure 11. Experimental results for the viscosity of supercritical SF_6 at 325 K. The free-decay data are systematically lower than the resonance-scan data at densities above 800 kg m^{-3}. At that density the deviation is about 6%.

integrating the data acquisition board in the computer so that electromagnetic interference is minimized. The present results suggest that free-decay measurements are advantageous at low densities to avoid parasitic modes of the crystal vibration. These may be excited in forced-mode measurements if the drive voltage cannot be lowered sufficiently due to hardware constraints between drive voltage and impedance resolution.

5. Nonlinear effects

5.1. Observations of the torsionally vibrating crystal

As discussed in section 4.1, the vacuum characterization of the crystal vibration revealed several interesting phenomena. Asymmetric resonance curves with resonant frequency shifts and decreases of the conductance maxima with increasing drive voltage were observed in this work. The conductance curves are skewed to lower frequencies and their maxima decrease with increased forcing at constant temperature. These effects are fundamentally the same as those which have been described for other crystal cuts and piezoelectric materials [23]. In the context of quartz resonators with high-frequency stability, the shift of the resonant frequency with amplitude is known as the amplitude–frequency effect [24].

In the free-decay measurements, similar phenomena have been observed. Sample free-decay data are shown in figures 9 and 10 and were discussed in section 4.1. The two observations in the free mode are a decrease of the resonant frequency and an increase of the apparent damping with increasing drive voltage. These observations are not consistent with the linearity of the crystal vibration on which the working theory of the viscometer is based. At amplitudes above a certain threshold, the torsional deformation of the crystal follows a nonlinear stress–strain relationship. In fact, measuring the shift of the resonant frequency due to the applied electric field allows the determination of the nonlinear, third-order piezoelectric coefficient d_{311} [25]. In the following, the nonlinear characteristics will be discussed in view of how they change the dissipation of the vibrator rather than in view of the material properties of the crystal. The dissipation of the vibrator is of interest for accurate viscosity measurements.

5.2. Generalized nonlinear oscillators

The asymmetric resonance, shift in f^*, possible hysteresis, change in maximum conductance, and variable damping are explained by considering Duffing and Van der Pol oscillators. Such oscillators exhibit displacement-dependent stiffness and damping, respectively. Their characteristics are discussed and analysed in detail by Thompson and Stewart [26], Moon [27], and others. The generalized equation of motion for these two types of forced oscillator is

$$I\frac{\mathrm{d}^2\theta}{\mathrm{d}t^2} + b\left(1+\frac{\alpha}{b}\theta^2\right)\frac{\mathrm{d}\theta}{\mathrm{d}t} + k\left(1+\frac{\gamma}{k}\theta^2\right)\theta = F\exp(\mathrm{j}\omega t). \quad (4)$$

Here, damping and stiffness are functions of the displacement θ. The constants α and γ represent the nonlinearities of Van der Pol and of Duffing oscillators respectively. In the fully generalized case, the inertia I may be displacement-dependent too [18]. Examples of oscillating systems with displacement-dependent inertia are the inertial cavitation of gas bubbles [28] or oscillations of thermally pumped vapour bubbles [29]. The displacement dependences of stiffness and damping are introduced in equation (4) as a Taylor series truncated to the quadratic term (θ^2). The expansion contains only even powers, which follows from symmetry arguments. If the oscillating system is symmetric with respect to the equilibrium position then the displacement dependence can include only even powers. Equation (4) reduces to the Duffing oscillator for $\alpha = 0$, and to the Van der Pol oscillator for $\gamma = 0$. Both effects may be coupled because of the material properties. However, in theory they may exist separately.

The following discussion presents a simple treatment of these nonlinear oscillators in the frequency domain. The two nonlinearities will be treated separately to discern which effects arise from which type of oscillator. By such an analysis, the observed behaviour of the torsionally vibrating crystal can be interpreted.

The Duffing oscillator is considered first assuming $\alpha = 0$. Its displacement-dependent *stiffness* is governed by the value of the constant γ. If $\gamma > 0$, the stiffness of the system increases with increasing amplitude, and the resonance curve is skewed to the right. If $\gamma < 0$, the stiffness of the system decreases with increasing amplitude and the resonance curve is asymmetric to the left. The linear harmonic oscillator is recovered in the case $\gamma = 0$ and the resonance curve is symmetric. Thus, the Duffing oscillator is evidenced by pronounced asymmetry of the resonance curve and a substantial shift in the resonant frequency. This behaviour has been observed in this work in the frequency response of the torsionally vibrating crystal. However, numerical analyses show that the Duffing oscillator does not exhibit a significant increase in bandwidth or a decrease in maximum conductance with increased forcing.

Figure 12 shows dissipation responses of a Duffing oscillator as a function of frequency calculated on the basis of equation (4). The dissipation $\langle\Pi\rangle$ is normalized by F^2 to show the effect on the impedance due to the Duffing effect. The figure compares results of an approximate solution outlined by Ku [30] with the numerical integration of Duffing's differential

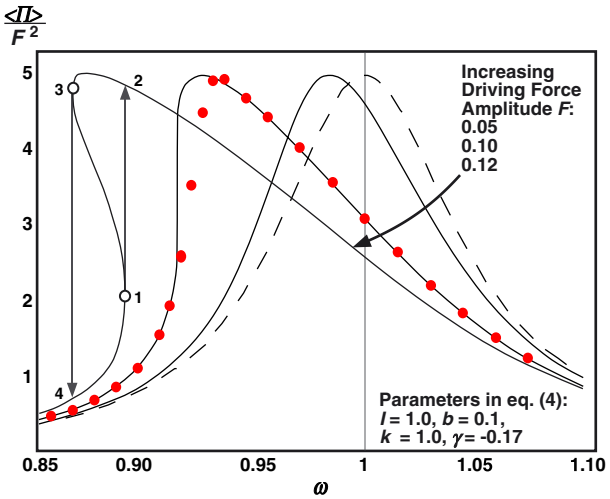

Figure 12. Normalized steady-state dissipation of a Duffing oscillator for external sinusoidal forcing calculated with the approximation of Ku [30]. The response is shown for three different forcing levels and the limit of zero forcing (the linear oscillator, dashed curve). The progress from symmetry, to asymmetry, and to hysteresis is shown. The points represent the numerical solution to the differential equation at a driving force of 0.10. The resonant frequency of the linear oscillator is 1.

equation. Although the numerical integration differs from the approximation of Ku at several points, the figure shows that the Duffing nonlinearity dramatically affects the frequency of maximum dissipation (i.e. the resonant frequency of a linear oscillator) and the asymmetry of the curve when the driving force increases. However, the maximum ($\langle\Pi\rangle F^{-2}$), corresponding to the maximum conductance $G_{\max}$ in the measurements with torsional crystals, is not changed.

Included in figure 12 is a calculated resonance for the forcing amplitude $F = 0.12$ which exhibits a region of multiple solutions. A hysteresis of a vibrator's frequency response would be observed in that region. When a scan starts at low frequency, the amplitude increases slowly until it reaches point 1. At this point, the amplitude of the oscillator jumps rapidly to point 2 and continues from there when the frequency is increased further. Conversely, when a scan starts at high frequencies, the amplitude increases with decreasing frequency until it reaches point 3 where it drops to point 4. These jumps are an expression of the multiplicity of the nonlinear differential equation of motion, equation (4). Thus, hysteresis can be observed in a Duffing oscillator when the forcing F exceeds a certain critical threshold. Below this critical forcing threshold, the system does not exhibit hysteresis but only an asymmetry of the resonance curve. This corresponds to the available amplitudes in the torsional crystals viscometer with the present instrumentation. Pronounced hysteresis was observed in this laboratory in a vibrating wire transducer [31] which has a much lower stiffness than quartz crystals. It may be possible to observe hysteresis of the torsionally vibrating crystal at higher forcing amplitudes than can be applied with the present instrumentation.

The Van der Pol nonlinearity, on the other hand, modifies the *damping* of the system with the term α so that it depends on the displacement of the oscillator. If $\alpha < 0$, the damping of the system decreases with increasing displacement. Conversely, if $\alpha > 0$ the damping of the system increases with displacement. As with the Duffing oscillator, if $\alpha = 0$ the resonance curve is unchanged. However, the frequency-domain effects of the Van der Pol nonlinearity are different from those of the Duffing nonlinearity. The most pronounced example of this is the 'relaxation oscillator' which exhibits self-excited oscillations [18] for certain values of $\alpha < 0$. In the case of small $\alpha > 0$, the resonance curve is flattened with a resultant higher apparent bandwidth. In addition, the resonant frequency shifts very slightly higher. Thus, the Van der Pol oscillator is evidenced by a decrease in the maximum conductance and a pronounced increase in measured damping. Both of these effects occur in the resonance scans of the torsional crystal oscillator. Also, the increase in damping with amplitude is obvious in the free-decay measurements (see figure 9). The crystal exhibits a linear response up to a displacement corresponding to an induced voltage of 200 mV *in vacuo*, after which the apparent damping increases substantially. This characteristic of the torsionally vibrating crystal is commensurate with a displacement-dependent damping according to the Van der Pol nonlinearity.

In summary, the nonlinear behaviour of the torsional crystal viscometer seems to be described by a combination of the Duffing and of the Van der Pol nonlinearity. The Duffing effect ($\gamma < 0$) is apparent in the pronounced asymmetry of the resonance curve, the shift in resonant frequency and the possible hysteresis. The Van der Pol characteristic is evidenced by the increase in damping and decrease in conductance at higher displacements ($\alpha > 0$).

6. Conclusions and perspectives

This work presents substantial progress toward accurate free-decay measurements in the torsional crystal viscometer. This method has several advantages compared with conventional resonance scans. It allows for measurements at smaller torsional displacements which ensures that the deduced viscosity is independent of the applied equilibrium perturbation [32]. Applying smaller torsional displacements is a prerequisite to extend the operating range of the instrument to routine measurements in gases. Since the amplitude of the crystal vibration is monitored directly, measurements of the external damping in fluids can be matched with the correct internal damping as determined *in vacuo*. This is particularly valuable for absolute viscosity measurements. The mutual validation of time- and frequency-domain measurements allows for a more complete characterization of the instrument and testing of its theory of operation [33]. Using these capabilities it may be possible to develop the torsional crystal viscometer into a primary instrument for the measurement of viscosity standards. The measurement range of the free-decay technique in fluid is currently smaller than that of the forced-mode technique. However, with improved signal conditioning and instrumentation this limit can be increased substantially. The rapid advance of computer technology with regard to processor speed and available memory increases the feasibility of free-decay measurements further.

For the first time, the nonlinear range of operation of this viscometer type has been explained. The observed nonlinear effects of the crystal oscillation have been interpreted in terms of Duffing and Van der Pol oscillators, which exhibit displacement-dependent stiffness and damping. This novel insight extends the understanding of torsional crystal viscometers.

The progression of the torsional crystal viscometer from a steady-state method (forced mode measurement) to a transient method (free-decay measurement) is analogous to the development of hot-wire instruments for thermal conductivity measurements of fluids. Initially, these were used in a steady-state mode with a stationary temperature gradient across the fluid [34]. As data acquisition capabilities increased, it became possible to monitor the transient temperature rise of the wire in response to a 1 s heat pulse [35, 36], while steady-state measurements required equilibration times on the order of hours. Due to this accelerated measurement mode, transient hot-wire instruments have become a *de facto* standard technique for thermal conductivity measurements of fluids. Similar advantages may be gained with the free-decay measurement technique in torsional crystal viscometers. They appear particularly attractive as an alternative method for the ubiquitous capillary viscosity measurements in industry.

Acknowledgments

R F Hafer was supported by the National Institute of Standards and Technology (NIST) Professional Research Experience Program (PREP). Thanks are due to Torsten Lüddecke (Hannover, Germany) and Dr Thomas Geers (University of Colorado at Boulder) for their respective help in understanding the mechanical behaviour of the crystal transducer. Acknowledgment is due to Lars Aumann for calling attention to and stimulating conversation about Duffing and Van der Pol oscillators. The constructive comments of the anonymous reviewers of this manuscript are greatly appreciated.

References

[1] Kestin J and Wakeham W 1988 Transport properties of fluids *Thermal Conductivity, Viscosity, and Diffusion Coefficient* (New York: Hemisphere)

[2] Diller D E 1991 Torsional crystal viscometer *Measurement of the Transport Properties of Fluids* 1st edn, ed J V Sengers (Oxford: Blackwell) pp 89–94

[3] Meyer H 1991 Low-temperature measurement *Measurement of the Transport Properties of Fluids* 1st edn, ed J V Sengers (Oxford: Blackwell) pp 390–426

[4] Gundrum J 1991 Entwicklung eines Quarzviskosimeters für Messungen bei hohen Temperaturen und Drücken *Dr.-Ing. Thesis* Technical University Clausthal, FRG

[5] Gualtieri J G 1989 Sweeping quartz crystals *IEEE 1989 Ultrasonics Symp.* ed B R McAvoy (Montréal, CA: IEEE) pp 381–91

[6] Meier K 1994 Observation and modeling of polar fluid behavior in a torsionally oscillating crystal viscometer *Study Thesis* Universität Hannover, FRG, and National Institute of Standards and Technology, Boulder, CO

[7] Eisele K M and Hollis Hallett A C 1958 The viscosity of liquid helium at frequencies of 11.8 and 35.5 kc/sec *Can. J. Phys.* **36** 25–34

[8] Betts D S, Osborne D W, Welber B and Wilks J 1963 The viscosity of liquid ^{3}He *Phil. Mag.* **8** 977–87

[9] Betts D S and Wilks J 1965 The viscosity of liquid ^{3}He above 0.04 K *9th Int. Conf. on Low Temp. Phys.* (New York: Plenum) pp 129–32

[10] Betts D S 1967 The effect of pressure on transport in semi-degenerate ^{3}He and ^{4}He *10th Int. Conf. Low Temp. Phys.* pp 178–83

[11] Bertinat M P, Betts D S, Brewer D F and Butterworth G J 1972 Effective viscosity of dilute solutions of liquid ^{3}He in ^{4}He between 20 mK and 1 K *Phys. Rev. Lett.* **28** 472–4

[12] Steward W G and Wallace G H 1971 He^4 viscosity measurements, 4 to 20 K, 0 to 10 MN m^{-2} *NBS report 10704* (Boulder, CO: National Bureau of Standards)

[13] Webeler R W H 1961 Viscosity × density measurements for normal liquid hydrogen and various ortho–para mixtures *PhD Thesis* University of Cincinnati

[14] Rouse P E Jr 1953 Viscoelastic properties of dilute polymer solutions *J. Appl. Phys.* **24** 690–6

[15] Bode B 1984 Entwicklung eines Quarzviskosimeters für Messungen bei hohen Drücken *Dr.-Ing. Thesis* Technical University Clausthal, FRG

[16] Richardson S M 1988 *Torsionally Vibrating Crystal Viscometer* (London: Imperial College) unpublished

[17] Kinsler L E, Frey A R, Coppens A B and Sanders J V 1982 *Fundamentals of Acoustics* 3rd edn (New York: Wiley)

[18] Den Hartog J P 1947 *Mechanical Vibrations* 3rd edn (New York: McGraw-Hill)

[19] Blanke W, Klingenberg G and Weiß R 1993 Thermische Zustandsgrößen von SF_6 auf der Dampfdruckkurve zwischen Tripelpunkt und dem kritischen Punkt sowie im Einphasengebiet zwischen 225 K und 450 K *PTB-Mitt.* **103** 27–35

[20] Wagner W, Kurzeja N and Pieperbeck B 1992 The thermal behaviour of pure fluid substances in the critical region—experiences from recent $p\rho T$ measurements on SF_6 with a multi-cell apparatus *Fluid Phase Equilib.* **79** 151–74

[21] Hafer R F 1999 Torsional crystal viscometry: wide-ranging resonance measurements and feasibility study of transient-decay measurements *MSc Thesis* Dept. of Chem. Eng., University of Colorado

[22] Taylor B N and Kuyatt C E 1994 Guidelines for evaluating and expressing the uncertainty of NIST measurement results NIST TN 1297 *Technical Note* (Washington, DC: National Institute of Standards and Technology)

[23] Sorge G, Beige H and Scheiding C 1985 Electromechanical resonances for investigations of structural phase transitions *Piezoelectricity* ed L A T Shuvalov and W George (New York: Gordon and Breach) pp 105–14

[24] Planat M and Hauden D 1985 Nonlinear properties of bulk and surface acoustic waves in piezoelectric crystals *Piezoelectricity* ed L A T Shuvalov and W George (New York: Gordon and Breach) pp 277–96

[25] Beige H and Schmidt G 1985 Electromechanical resonances for investigating linear and nonlinear properties of dielectrics *Piezoelectricity* ed L A T Shuvalov and W George (New York: Gordon and Breach) pp 93–103

[26] Thompson J M T and Stewart H B 1986 *Nonlinear Dynamics and Chaos—Geometrical Methods for Engineers and Scientists* (Chichester: Wiley)

[27] Moon F C 1987 *Chaotic Vibrations: an Introduction for Applied Scientists and Engineers* (New York: Wiley)

[28] Apfel R E 1997 Sonic effervescence: a tutorial on acoustic cavitation *J. Acoust. Soc. Am.* **101** 1227–37

[29] Feng Z C and Leal L G 1997 *Nonlinear Bubble Dynamics Annual Review of Fluid Mechanics* (Palo Alto, CA: Annual Reviews Inc.) pp 201–43

[30] Ku I-C 1958 *Analysis and Control of Nonlinear Systems: Nonlinear Vibrations and Oscillations in Physical Systems* (New York: Ronald Press)

[31] Aumann L 1999 Calibration of a vibrating-wire viscometer for mixtures of ammonia and water *Dipl.-Ing. Thesis* Universität Hannover, FRG, and National Institute of Standards and Technology, Boulder, CO

[32] Wilhelm J, Vogel E, Lehmann J K and Wakeham W A 1998 A vibrating-wire viscometer for dilute and dense gases *Int. J. Thermophys.* **19** 391–401

[33] Gillis K A, Mehl J B and Moldover M R 1996 Greespan acoustic viscometer for gases *Rev. Sci. Instrum.* **67** 1850–7

[34] Le Neindre B, Tufeu R and Sirota A M 1991 Steady-state methods for thermal conductivity *Measurement of the Transport Properties of Fluids* 1st edn, ed J V Sengers (Oxford, UK: Blackwell) pp 113–60

[35] Healy J J, de Groot J J and Kestin J 1976 The theory of the transient hot-wire method for measuring thermal conductivity *Physica* C **82** 392–408

[36] Roder H M 1981 A transient hot wire thermal conductivity apparatus for fluids *J. Res. Natl Bur. Stand.* **86** 457–93